

InfiniDreamer: Arbitrarily Long Human Motion Generation via Segment Score Distillation

Wenjie Zhuo, Fan Ma, Hehe Fan
 ReLER Lab, CCAI, Zhejiang University
 wenjiezhuo@zju.edu.cn

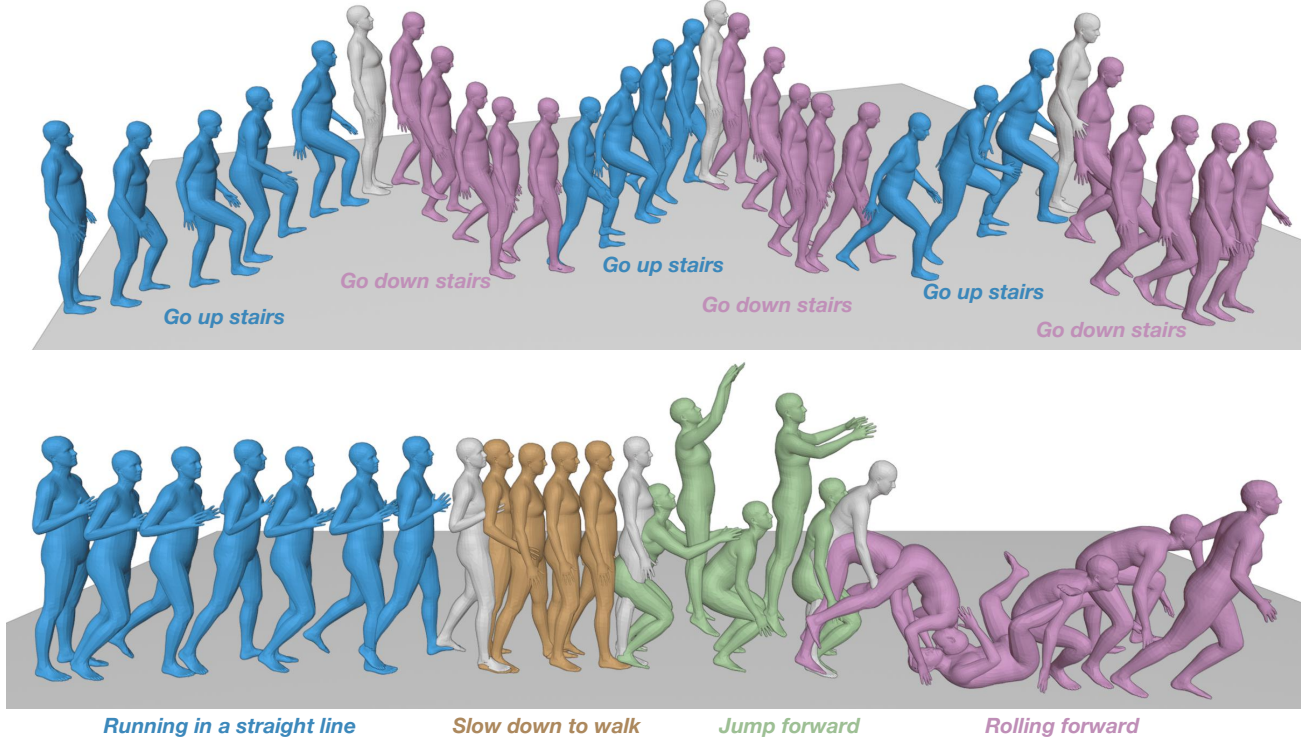


Figure 1. **Long motion sequences generated by InfiniDreamer.** Given a list of textual prompts, our framework generates realistic human motions corresponding to each prompt, along with smooth and coherent transitions between them. This approach ultimately synthesizes a continuous, fluid long-duration human motion without requiring any long sequence data.

Abstract

We present *InfiniDreamer*, a novel framework for arbitrarily long human motion generation. *InfiniDreamer* addresses the limitations of current motion generation methods, which are typically restricted to short sequences due to the lack of long motion training data. To achieve this, we first generate sub-motions corresponding to each textual description and then assemble them into a coarse, extended sequence using randomly initialized transition segments. We then introduce an optimization-based method called *Segment Score Distillation (SSD)* to refine the entire long motion sequence. *SSD* is designed to utilize an existing motion prior, which is trained only on short clips, in a training-free manner. Specifically, *SSD* iteratively refines

overlapping short segments sampled from the coarsely extended long motion sequence, progressively aligning them with the pre-trained motion diffusion prior. This process ensures local coherence within each segment, while the refined transitions between segments maintain global consistency across the entire sequence. Extensive qualitative and quantitative experiments validate the superiority of our framework, showcasing its ability to generate coherent, contextually aware motion sequences of arbitrary length.

1. Introduction

This paper focuses on arbitrarily long 3D human motion generation [2, 3, 8, 23, 44, 62]. It is a challenging task

in computer vision, with great potential to benefit various downstream applications, such as AR/VR and film production. Benefiting from advancements in deep generative models [4, 10, 17, 33, 41, 46] and the availability of large text-to-motion datasets [12, 13, 30, 36, 38], text-to-motion generation has seen significant progress. Recent approaches [1, 6, 9, 14, 20, 35, 49, 56–59] are capable of generating realistic and coherent short motion sequences, typically around 10 seconds in duration. However, in most real-world applications, such as long-duration animations in gaming [18] and full-body motion capture [28, 53], much longer motion sequences, spanning minutes or even hours, are often required. This gap presents a significant barrier to the broader applicability of current methods and highlights the critical need for advancements in generating continuous long-duration motions.

The primary challenge in generating arbitrarily long-motion sequences lies in the limited availability of high-quality long-sequence data [15, 25, 26, 38, 39]. Most existing datasets predominantly consist of short sequences annotated with single actions [12, 38] or simple textual descriptions [13, 30, 36], lacking the temporal depth needed for continuous long-motion generation. To overcome these limitations, many previous works adopted auto-regressive models [2, 23, 26, 39], which generate motions step-by-step based on previously generated frames. However, this auto-regressive nature often leads to the accumulation of errors over time, resulting in issues such as motion drift, repetitive patterns, and discontinuities over long motion sequences. Alternatively, some works utilize the infilling capabilities of motion diffusion models [44, 54, 61]. In these methods, motion segments are generated based on individual textual descriptions, and transitions between segments are filled in through in-painting. However, due to the strong modifications applied at the boundaries of each segment, this approach often leads to conflicts between adjacent motions, causing abrupt transitions, distortions in movement, or even overwriting of previously generated content.

To mitigate the issues, we turn to a smoother synthesis approach based on score distillation. Originally introduced by DreamFusion [37], Score Distillation Sampling (SDS) [37] enables the creation of 3D assets using only a pre-trained text-to-image diffusion model. Unlike traditional diffusion sampling methods, which can result in abrupt local modifications, SDS [37] emphasizes a gradual and smooth distillation process that maintains coherence across different views. Extending this advantage to temporal generation opens new possibilities for producing coherent long-duration human motion.

In this paper, we propose **InfiniDreamer**, a novel framework for generating arbitrarily long motion sequences. By contextually fine-tuning each sub-motion and refining transition segments between sub-motions, InfiniDreamer can

generate coherent long-sequence motion in a training-free manner. Specifically, we first generate each sub-motion conditioned on its corresponding textual prompt and then assemble them into a coarsely extended sequence using randomly initialized transition segments. Next, we utilize a sliding window approach to iteratively sample short overlapping sequence segments from the coarse long motion sequence. We then propose **Segment Score Distillation (SSD)**, an optimization method that refines each short sequence segment by aligning it with the pre-trained motion prior. This segment-wise optimization ensures the local coherence of each sampled segment, while the refined transition segments maintain global consistency across the entire long motion sequence. After multiple rounds of optimization, our framework eventually yields coherent, contextually-aware long motion sequences. To verify the effectiveness of our framework, we evaluated the motion sequence and transition segments on two commonly used datasets, HumanML3D [13] and BABEL [38]. The experimental results show that our method is significantly better than the previous training-free method. We also demonstrate our framework qualitatively, and the results show that our method has great contextual understanding capabilities, enable a seamless, coherent synthesis of long-duration motion sequences.

Overall, our contributions can be summarized as follows:

- (1) We introduce InfiniDreamer, a novel framework capable of generating arbitrarily long human motion sequences in a training-free manner.
- (2) We propose Segment Score Distillation (SSD), which iteratively refines overlapping short segments sampled from the coarse long motion. This process aligns each segment with the pre-trained motion prior, ensuring local and global consistency across the entire motion sequence.
- (3) We conduct qualitative and quantitative evaluations of our framework. Experimental results show that our framework brings consistent improvement over the previous training-free methods.

2. Related Work

2.1. Text-to-Motion Generation

Text-to-motion generation [1, 6, 9, 14, 20, 35, 48, 49, 56–60, 65], which aims to create realistic human motions from textual descriptions, has gained substantial attention in recent years. Current works can be categorized into two main types: (i) GPT-based model and (ii) Diffusion-based Model. The former includes notable work such as T2M-GPT [57], which combines VQ-VAE [50] with a transformer architecture for human motion generation from text, achieving impressive results. MotionGPT [20] treats human motion as a foreign language and trains on a mixed motion-language dataset to build a unified motion-language model. Mo-

Mask [14] proposes a masked transformer framework with residual transformer, enhancing text-to-motion generation. On the other hand, diffusion-based models are first introduced by MotionDiffuse [58] and MDM [49]. They developed a transformer-based diffusion model for generating motion based on text input. Rather than directly mapping raw motion data to text, MLD [6] encodes motion into a latent space, improving the model’s efficiency. Recently, Motion Mamba [64] combines state-space models (SSMs) [11] with diffusion models, offering an efficient framework for text-to-motion generation. All of these methods are capable of generating realistic and coherent human motion sequences, yet producing arbitrarily long human motion remains a challenge.

2.2. Long Human Motion Generation

Long human motion generation [2, 8, 15, 23–26, 39, 40, 44, 54, 62–64] is essential for many practical applications but remains constrained by limited datasets. Previous methods like Multi-Act [23] and TEACH [2] utilize a recurrent generation framework, and generate motion conditioned on the previously generated motion segment and the corresponding text prompt. However, these models suffer from error accumulation over time, causing issues like motion drift, repetitive patterns, and even ‘freezing’ after several iterations. To overcome this limitation, PCMDM [54] introduces a past-conditioned diffusion model alongside a coherent sampling strategy for long human motion generation. PriorMDM [44] proposes an innovative sequential composition approach, which generates extended motion by composing prompted intervals and their transitions. FlowMDM [3] proposes Blended Positional Encodings for seamless human motion composition. Recently, M2D2M [8] introduces adaptive transition probabilities and a two-phase sampling strategy to produce smooth and realistic motion sequences. In this work, we introduce a score distillation method, which refines randomly sampled short segments by aligning them with a pre-trained motion diffusion prior. This process ultimately generates a coherent and smooth long motion sequence.

3. Preliminaries

3.1. Score Distillation Sampling

Score Distillation Sampling (SDS) was originally introduced in DreamFusion [37] for the task of text-to-3D generation [5, 7, 19, 21, 27, 37, 47, 52, 55, 66]. It leverages the probability density distillation from a text-to-image diffusion model [42] to optimize the parameters of any differentiable 3D generator, enabling zero-shot text-to-3D generation without requiring explicit 3D supervision. The flexibility of SDS allow it to guide various implicit representations like NeRF [31, 32], 3DGS [22] and image space [16, 43]

towards high-fidelity results.

Formally, SDS utilizes a pre-trained diffusion prior ϕ to guide the implicit representation parameterized by θ . Given a camera pose π , let $x = g(\theta; \pi)$ denote the image rendered from a differentiable rendering function g with parameter θ . SDS minimizes the density distillation loss between the posterior of $x = g(\theta; \pi)$ and the conditional density $p_\phi(x_t; y, t)$, which is a variational inference via minimizing KL divergence:

$$\min_{\theta} \mathcal{L}_{SDS}(\theta; x) = \mathbf{E}_{t, \epsilon} \left[\frac{\alpha_t}{\sigma_t} D_{KL}(q(x_t | g(\theta; \pi)) || p_\phi(x_t; y, t)) \right], \quad (1)$$

where $x_t = \alpha_t x + \sigma_t \epsilon$ with $\epsilon \sim \mathcal{N}(0, I)$. They further derive SDS by differentiating Eq. 1 with respect to differentiable generator parameter θ , and omitting the U-Net Jacobian term to reduce computational cost and enhance performance. The SDS gradient update is given as follows:

$$\nabla_{\theta} \mathcal{L}_{SDS}(\theta; x) = \mathbf{E}_t [w(t)(\epsilon_\phi(x_t; y, t) - \epsilon) \frac{\partial x}{\partial \theta}]. \quad (2)$$

Previous works have demonstrated the effectiveness of score distillation loss in areas such as 3D generation [37, 51], image editing [16] and video editing [67]. However, its application remains largely unexplored in other fields. In this work, we take a pioneering step by introducing Score distillation into the domain of long-sequence human motion generation, extending its utility to this challenging task.

4. Methodology

4.1. Problem Definition

Long-sequence human motion generation refers to the task of producing continuous and coherent motion sequences over extended time durations. Specifically, given a series of textual conditions $Y = \{y_1, y_2, y_3, \dots, y_n\}$ as input, our goal is to generate the corresponding long-motion sequence $M = \{m_1, t_1, m_2, t_2, \dots, m_n\}$, where m_i represents the motion corresponding to each text prompts y_i , and t_i denotes the transition segments between consecutive motion sequences m_i and m_{i+1} . This task requires that each sub-sequence m_i aligns closely with the corresponding textual condition y_i . In other words, the generated motion should accurately reflect the intent and meaning of each prompt. At the same time, each transition segment t_i should feel as realistic and natural as possible. This ensures smooth transitions between the motion segments m_i and m_{i+1} , allowing for a seamless flow in the overall motion sequence.

4.2. InfiniDreamer

As shown in Fig. 2, Our proposed method, InfiniDreamer, consists of three main modules:

- **Motion Sequence Initialization Module.** The first stage in our framework is the initialization of the long motion

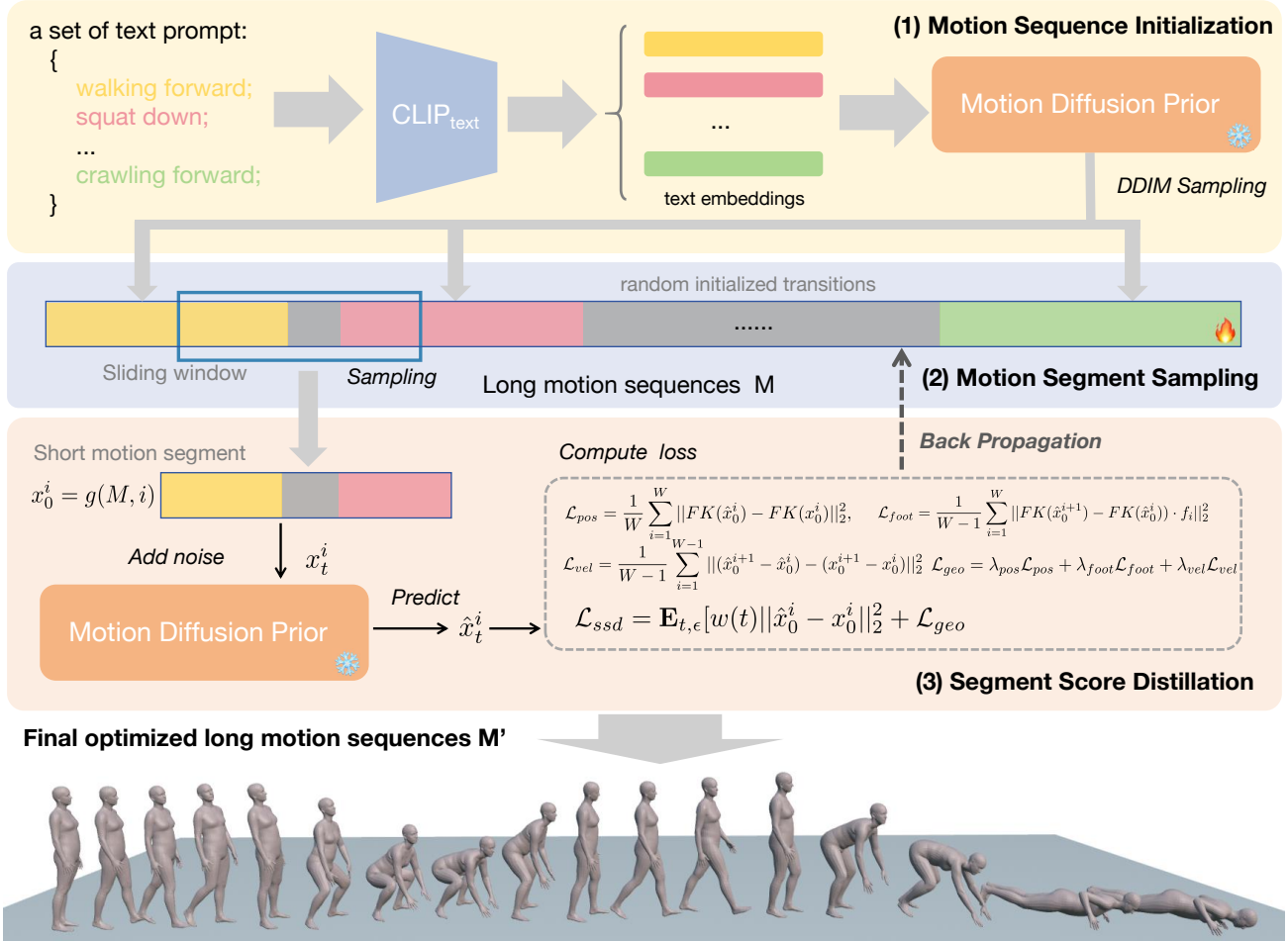


Figure 2. **Overview of InfiniDreamer** for arbitrarily long human motion generation. Given a list of text prompts, our framework generates a coherent and continuous long-sequence motion that aligns closely with each prompt. To achieve this, we start by initializing a long motion sequence using the (1) **Motion Sequence Initialization** module. Next, the (2) **Motion Segment Sampling** module iteratively samples short, overlapping sequence segments from the initialized motion. Finally, we refine each sampled segment with our proposed (3) **Segment Score Distillation**, optimizing each segment to align with the prior distribution of the pre-trained motion diffusion model. Through this iterative process, the framework synthesizes a seamless and fluid long-duration motion sequence, with realistic motions matching each prompt and smooth transitions connecting them.

sequence, serving as a foundational structure for further optimization. To create this initial sequence, we start by randomly initializing the entire long motion sequence M , which provides a rough, unsmoothed outline of the target motion. Then, we employ a pre-trained Motion Diffusion Model (MDM) [49] with DDIM sampling [46] to generate each motion segment m_i within the sequence. Each segment m_i is conditioned on the respective text prompt y_i , ensuring that the generated motion aligns semantically with the desired motion described in the prompt.

• **Motion Segment Sampling Module.** With the initialized sequence in place, we proceed to sample specific motion segments, which are essential for guiding the iterative optimization in subsequent steps. To achieve this, we employ a sliding window of size W , which moves along the long

motion sequence with a stride size S . This sliding window technique allows us to iteratively sample overlapping short motion segments from the long sequence, denoted as x_0^i . By maintaining overlap between adjacent segments, the sliding window preserves continuity and smoothness between them, thereby enhancing the temporal coherence of the generated long motion sequence.

• **Segment Score Distillation.** This module leverages a pre-trained motion diffusion model ϕ to optimize the distribution of the sampled short sequences, ensuring that each segment aligns with the underlying diffusion sample distribution. Specifically, Segment Score Distillation (SSD) iteratively optimizes each short motion segment to bring it closer to the high-quality distribution learned by the diffusion model, thereby enhancing the coherence and quality

of the overall long motion sequence. To achieve this, for each sampled short motion segment x_0^i , we first randomly sample a timestep $t \sim \mathcal{U}(20, 980)$, then obtain each noised segment x_t^i through $x_t^i = \sqrt{\alpha_t}x_0^i + \sqrt{\sigma_t}\epsilon$, where α_t and σ_t are noise scheduling parameters, and ϵ represents Gaussian noise.

Using the motion diffusion model in an unconditional setting, we then incorporate an alignment loss to align the sampled motion segment with the predicted signal $\hat{x}_0^i = \phi(x_t^i; t, \emptyset)$:

$$\mathcal{L}_{align} = \mathbf{E}_{t, \epsilon} [w(t) \|\hat{x}_0^i - x_0^i\|_2^2], \quad (3)$$

where $w(t)$ is weighting function. To further improve the coherence and realism of generated motions, we augment our method with three commonly used geometric losses, inspired by prior work [34, 45, 49]. These include (1) positional constraints when predicting rotations, (2) foot contact constraints to maintain stable ground interaction, and (3) velocity regularization to encourage smooth transitions:

$$\mathcal{L}_{pos} = \frac{1}{W} \sum_{i=1}^W \|FK(\hat{x}_0^i) - FK(x_0^i)\|_2^2, \quad (4)$$

$$\mathcal{L}_{foot} = \frac{1}{W-1} \sum_{i=1}^W \|FK(\hat{x}_0^{i+1}) - FK(\hat{x}_0^i) \cdot f_i\|_2^2, \quad (5)$$

$$\mathcal{L}_{vel} = \frac{1}{W-1} \sum_{i=1}^{W-1} \|(\hat{x}_0^{i+1} - \hat{x}_0^i) - (x_0^{i+1} - x_0^i)\|_2^2, \quad (6)$$

where $FK(\cdot)$ is the forward kinematic function, it maps joint rotations to joint positions (or acts as the identity function if joint rotations are not predicted). $f_i \in \{0, 1\}^J$ is the binary foot contact mask for each frame i , it denotes whether the foot touches the ground, helping mitigate foot-sliding by nullifying ground-contact velocities. Together, our final Segment Score Distillation loss is:

$$\mathcal{L}_{ssd} = \mathcal{L}_{align} + \lambda_{pos}\mathcal{L}_{pos} + \lambda_{foot}\mathcal{L}_{foot} + \lambda_{vel}\mathcal{L}_{vel}, \quad (7)$$

where λ_{pos} , λ_{foot} and λ_{vel} are hyper-parameters that balance the contribution of each geometric loss in the overall objective function. We set them to 0 in our experiments on the HumanML3D dataset and set them to 0.1 for the BABEL dataset. We summarize our proposed SSD in Algorithm 1.

5. Experiments

5.1. Datasets

We evaluate InfiniDreamer on two datasets, HumanML3D [13] and BABEL [38], which are essential benchmarks for assessing motion generation models.

HumanML3D. The HumanML3D dataset [13] consists of 14,616 motion samples, each paired with 3-4 textual descriptions, enabling the model to learn from rich, multi-perspective annotations. These motions are sampled at

Algorithm 1 Segment Score Distillation (SSD)

Require: Initial motion sequence M_0 , motion diffusion model ϕ , number of iteration N , windows size W , stride S , learning rate η

Ensure: Optimized long motion sequence M

- 1: **Initialize:** $M \leftarrow M_0$
 - 2: **for** $n = 1$ to N **do**
 - 3: Sample a start index i from $\{1, 1 + S, \dots, \text{len}(M) - W\}$
 - 4: Extract a motion segment $x_0^i \leftarrow M[i : i + W]$
 - 5: Sample a timestep $t \sim \mathcal{U}(20, 980)$
 - 6: Add noise to obtain $x_t^i = \sqrt{\alpha_t}x_0^i + \sqrt{\sigma_t}\epsilon$, where $\epsilon \sim \mathcal{N}(0, I)$
 - 7: Compute total SSD loss via Eq. 7
 - 8: Update M by backpropagating \mathcal{L}_{ssd} and adjusting the values of x_0^i in M
 - 9: **end for**
 - 10:
 - 11: **return** Optimized long motion sequence M
-

20 FPS and derive from the AMASS [30] and HumanAct [12] datasets, with additional manual text descriptions for greater semantic detail. HumanML3D utilizes a 263-dimensional pose vector that encodes joint coordinates, angles, velocities, and feet contact information, allowing for precise motion modeling. For evaluation, we use motions with lengths ranging from 40 to 200 frames.

BABEL. The BABEL dataset [38] consists of 10,881 sequential motion samples and a total of 65,926 segments, wherein each segment correlates with a distinct textual annotation. This high level of segmentation supports the modeling of nuanced transitions and distinct action phases, making BABEL a valuable benchmark for evaluating long-motion generation. During evaluation, we follow the setting of PriorMDM [44], which refines BABEL by excluding poses like ‘a-pose’ or ‘t-pose’ and combines transitions with subsequent actions to create smoother sequences.

5.2. Implementation details

We use the Motion Diffusion Model (MDM) [49] as our short motion prior. For HumanML3D, we use the pre-trained model with 0.6M steps trained on this dataset, while for BABEL, we use the pre-trained model with 1.25M steps. For the optimization process, we set the guidance scale as 7.5 and sample time steps $t \sim \mathcal{U}(20, 980)$. For all results, we set the patch size as 60 and the stride size as 30. We optimized all long motion sequences for 20000 iterations using AdamW [29] optimizer with a learning rate 0.002. We conduct all experiments on a single A6000 GPU.

	Motion				Transition (30 frames)	
	R-precision \uparrow	FID \downarrow	Diversity \rightarrow	MultiModal-Dist \downarrow	FID \downarrow	Diversity \rightarrow
Ground Truth	0.797 ± 0.003	$1.6 \cdot 10^{-3} \pm 0.00$	9.59 ± 0.13	2.98 ± 0.01	$1.8 \cdot 10^{-3} \pm 0.00$	9.55 ± 0.09
DoubleTake [44]	0.603 ± 0.009	1.36 ± 0.03	9.33 ± 0.15	4.27 ± 0.01	<u>3.19 ± 0.29</u>	<u>8.09 ± 0.08</u>
DiffCollage [61]	<u>0.605 ± 0.006</u>	<u>1.07 ± 0.05</u>	<u>9.34 ± 0.11</u>	<u>3.62 ± 0.01</u>	4.27 ± 0.09	7.47 ± 0.08
InfiniDreamer (ours)	0.627 ± 0.009	0.62 ± 0.07	9.60 ± 0.15	3.37 ± 0.01	2.43 ± 0.30	8.44 ± 0.09

Table 1. Comparison of InfiniDreamer with the state of the art in HumanML3D. Symbols \uparrow , \downarrow , and \rightarrow mean that higher, lower, or closer to the ground truth (GT) value are better, respectively. We run each evaluation 10 times to obtain the final results. We use **Bold** to indicate the best result, and use underline to indicate the second-best result.

	Motion				Transition (30 frames)	
	R-precision \uparrow	FID \downarrow	Diversity \rightarrow	MultiModal-Dist \downarrow	FID \downarrow	Diversity \rightarrow
Ground Truth	0.629 ± 0.001	$0.4 \cdot 10^{-3} \pm 0.00$	8.52 ± 0.09	3.51 ± 0.01	$0.7 \cdot 10^{-3} \pm 0.00$	8.23 ± 0.14
TEACH [2]	0.461 ± 0.012	1.43 ± 0.04	7.71 ± 0.11	7.93 ± 0.01	4.23 ± 0.37	8.37 ± 0.11
DoubleTake [44]	0.483 ± 0.009	<u>1.14 ± 0.05</u>	8.28 ± 0.09	6.97 ± 0.01	3.54 ± 0.10	7.31 ± 0.12
DiffCollage [61]	0.487 ± 0.009	1.83 ± 0.05	7.89 ± 0.11	6.74 ± 0.01	4.62 ± 0.09	7.07 ± 0.08
InfiniDreamer (ours)	0.522 ± 0.008	<u>1.14 ± 0.11</u>	7.97 ± 0.05	<u>6.35 ± 0.01</u>	<u>2.43 ± 0.30</u>	7.63 ± 0.05
+ geo losses	<u>0.518 ± 0.008</u>	1.07 ± 0.09	<u>8.13 ± 0.08</u>	6.33 ± 0.01	2.27 ± 0.33	<u>7.95 ± 0.05</u>

Table 2. Comparison of InfiniDreamer with the state of the art in BABEL. Symbols \uparrow , \downarrow , and \rightarrow mean that higher, lower, or closer to the ground truth (GT) value are better, respectively. We run each evaluation 10 times to obtain the final results. We use **Bold** to indicate the best result, and use underline to indicate the second-best result.

5.3. Evaluation metrics

To evaluate our approach, we utilize the following metrics: (1) R-Precision which measures the semantic alignment between the input text and the generated motions. R-Precision measures the degrees to which generated motions align with the provided textual descriptions, while Multimodal Distance evaluates the consistency between multiple generated motions and the text. (2) Frechet Inception Distance (FID), which evaluates the overall quality of motions by comparing the distribution of high-level features between generated motions and real motions. A lower FID indicates a closer resemblance to real motions. (3) Diversity measures the variability and richness of the generated motion sequences. (4) The Multimodal Distance metric, which measures the diversity of motions generated from a single text prompt, indicates the model’s ability to generate varied interpretations of the same input.

5.4. Quantitative Comparisons

Following previous works [2, 44], we quantitatively evaluate the quality of generated long motion sequences on HumanML3D [13] and BABEL [38]. For motion sequences, we use R-precision, FID, Diversity, and Multimodal distance metrics to measure their quality, while for transition segments, we use FID and Diversity to measure their quality. As shown in Table 1 and Table 2, InfiniDreamer brings consistent improvement over the current state-of-the-

art methods. In HumanML3D, our framework outperforms previous methods across all evaluation metrics. The generated sequences demonstrate a higher degree of alignment with the input text and closely match the distribution of real data. Additionally, our framework achieves superior results in generating transition segments. In Babel, our framework achieves a significant advantage in R-precision, indicating better alignment between the generated motions and the textual descriptions. Furthermore, when we apply the geometric loss, our model demonstrates additional improvements in the FID metric, enhancing the realism and quality of the generated motion sequences.

5.5. Qualitative Comparisons

To further showcase the advantages of our approach, we conduct qualitative experiments to compare our method with DoubleTake [44]. We present two comparative experiments. In the upper row of Fig. 3, we use the prompts “a person walks forward slowly” and “a person slowly walks downstairs”. DoubleTake [44] exhibits motion drift in the transition segment between these motions, resulting in an overall lack of coherence. In contrast, our framework demonstrates strong contextual understanding, inferring an “walk upstairs” segment in response to the “walk downstairs” prompt. In the lower example, DoubleTake [44] shows issues with motion distortion and motion lost, while our framework successfully avoids these problems. Both

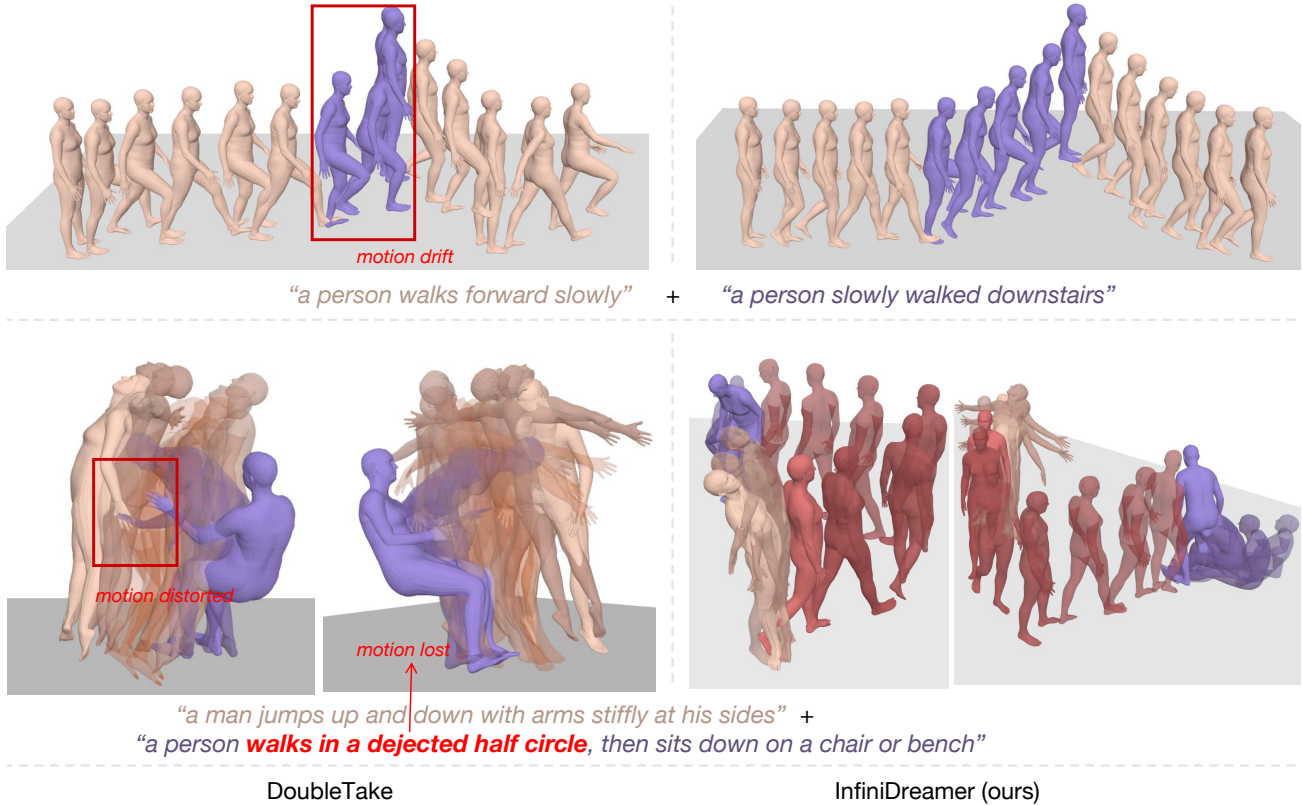


Figure 3. Qualitative Comparisons to Baseline for Long Motion Generation. We present two examples: in the top row, our framework demonstrates strong contextual understanding, guiding the transition segment to “go upstairs” in response to the following “downstairs” prompt. In contrast, the baseline shows motion drift in this segment. In the bottom row, we use a more fine-grained textual prompt, where the baseline method exhibits issues with motion distortion and motion loss, failing to generate the “walk in a dejected half circle” segment. Our framework, however, produces a higher-quality sequence with enhanced fine-grained comprehension of the text.

examples validate the superiority of our framework.

6. Ablation study

Ablation on Sliding Window Size W . In Tab. 3, we present the impact of the hyper-parameter Sliding Window Size W on model performance. W controls the size of each sampled segment, whereas a larger W allows the model to incorporate more contextual information. We observe that with a very small W , the performance of transition segments declines sharply. However, as W increases, the transition quality exhibits fluctuating declines. This suggests that a moderate context length is beneficial for transition generation, whereas an overly extended context introduces interference. In terms of motion segment generation, performance consistently decreases as W grows. We speculate this is due both to MDM’s limitations in handling long sequences and to the interference in semantic alignment caused by excessive context length.

Ablation on Stride Size P . In Tab. 3, we also examine the impact of the hyper-parameter Stride Size P on model

performance. P controls the frame shift of the sliding window in each step and, consequently, the overlap between segments. Our experiments show that when $P < W$, this parameter has minimal impact on performance. However, when $P \geq W$, there is a noticeable improvement in motion generation, whereas transition generation performance drops sharply.

The improvement in motion generation can be attributed to the nature of SSD, which adds noise during optimization. This noise slightly degrades motion quality. When $P \geq W$, certain motion frames are excluded from sampling and thus bypass SSD optimization, resulting in performance gains. In contrast, since transitions are initialized randomly, excluding certain transition frames from optimization effectively leaves them as random noise, which severely impacts transition quality.

Ablation on Learning Rate η . The learning rate η controls the update magnitude for long motion sequence parameters. In Fig. 4, we illustrate the effect of different learning rates on motion sequence generation. We observe that an excessively high learning rate will cause the motion amplitude

	Motion				Transition (30 frames)	
	R-precision \uparrow	FID \downarrow	Diversity \rightarrow	MultiModal-Dist \downarrow	FID \downarrow	Diversity \rightarrow
Ground Truth	0.797 ± 0.003	$1.6 \cdot 10^{-3} \pm 0.00$	9.59 ± 0.13	2.98 ± 0.01	$1.8 \cdot 10^{-3} \pm 0.00$	9.55 ± 0.09
$W = 30, P = 30$	0.632 ± 0.010	<u>0.45 ± 0.05</u>	9.48 ± 0.15	3.24 ± 0.01	3.97 ± 0.29	7.92 ± 0.09
$W = 60, P = 30$	0.627 ± 0.009	0.62 ± 0.07	9.60 ± 0.15	3.37 ± 0.01	2.43 ± 0.30	8.44 ± 0.09
$W = 90, P = 30$	0.618 ± 0.011	0.74 ± 0.07	9.59 ± 0.16	3.34 ± 0.01	2.53 ± 0.29	8.40 ± 0.08
$W = 120, P = 30$	0.605 ± 0.009	0.83 ± 0.08	<u>9.58 ± 0.16</u>	3.39 ± 0.01	<u>2.45 ± 0.30</u>	8.46 ± 0.09
$W = 150, P = 30$	0.586 ± 0.009	0.87 ± 0.07	9.50 ± 0.17	3.43 ± 0.01	2.63 ± 0.33	8.39 ± 0.09
$W = 60, P = 20$	0.625 ± 0.008	0.63 ± 0.09	9.56 ± 0.19	3.43 ± 0.01	2.53 ± 0.29	<u>8.45 ± 0.08</u>
$W = 60, P = 40$	0.626 ± 0.008	0.61 ± 0.08	9.48 ± 0.17	3.54 ± 0.01	2.58 ± 0.36	8.43 ± 0.09
$W = 60, P = 50$	0.623 ± 0.008	0.59 ± 0.09	9.57 ± 0.17	3.43 ± 0.01	2.63 ± 0.36	8.43 ± 0.08
$W = 60, P = 60$	0.625 ± 0.008	0.49 ± 0.07	<u>9.58 ± 0.09</u>	<u>3.31 ± 0.01</u>	3.54 ± 0.36	8.09 ± 0.15
$W = 60, P = 70$	<u>0.631 ± 0.010</u>	0.43 ± 0.07	9.58 ± 0.08	3.35 ± 0.01	3.69 ± 0.32	7.97 ± 0.14

Table 3. Ablation Study on Sliding Window Size W and Stride Size P . Experimental results show that as W increases, the alignment between individual motions and text decreases due to the addition of more contextual information. When $P \geq W$, some motion segments cannot be sampled, which has a negative impact on randomly initialized transition segments.

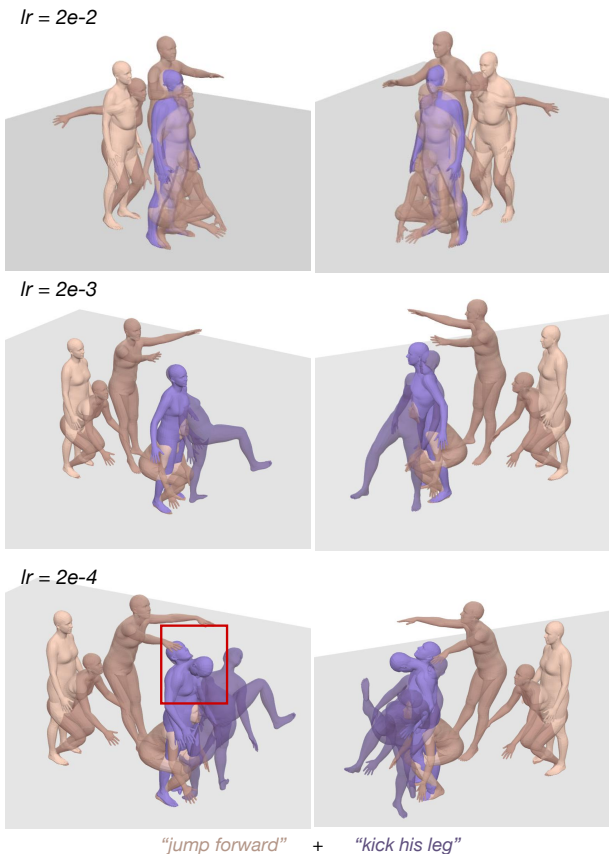


Figure 4. Ablation Study on Learning Rate η . We experiment with different η and find that an excessively high learning rate leads to motion stillness (*i.e.*, motion lost), while a lower learning rate results in large noise disturbances, causing motion distortions.

to gradually decrease, eventually resulting in a static output, leading to motion loss. As shown in the top row of Fig. 4, where a kicking motion is optimized into stillness. Conversely, a lower learning rate leads to under-training, introducing more noise and causing motion distortions. As shown in the bottom of Fig. 4, we notice significant motion distortion and exaggerated amplitude in the transitional phase preceding the kick motion, highlighting the need for a balanced learning rate.

7. Conclusion

In this paper, we present InfiniDreamer, a novel framework designed for generating arbitrarily long motion sequences from a list of textual descriptions. InfiniDreamer treats the long motion sequence as the differentiable parameters, and optimizes them using our proposed Segment Score Distillation (SSD), a method that employs pre-trained motion diffusion prior to optimize the short motion segment. Specifically, we iteratively sample short motion segments from the random initialized long-sequence motion. By continuously optimizing each sampled short motion segment from the long-sequence motion, we align each segment with the distribution of a pre-trained motion diffusion prior. This iterative process ultimately yields a coherent long-sequence motion. Note that our approach is independent of any specific motion diffusion prior. In other words, the generation of short motion clips and the ensemble of long motion sequences are decoupled. Therefore, future advancements in diffusion priors for short motion clip generation could further enhance the performance of our method. We hope our approach offers a new direction for addressing challenges in long-sequence generation.

References

- [1] Chaitanya Ahuja and Louis-Philippe Morency. Language2pose: Natural language grounded pose forecasting. In *2019 International Conference on 3D Vision (3DV)*, pages 719–728. IEEE, 2019. 2
- [2] Nikos Athanasiou, Mathis Petrovich, Michael J Black, and Gül Varol. Teach: Temporal action composition for 3d humans. In *2022 International Conference on 3D Vision (3DV)*, pages 414–423. IEEE, 2022. 1, 2, 3, 6
- [3] German Barquero, Sergio Escalera, and Cristina Palmero. Seamless human motion composition with blended positional encodings. In *Proceedings of the IEEE/CVF Conference on Computer Vision and Pattern Recognition*, pages 457–469, 2024. 1, 3, 2
- [4] Tom B Brown. Language models are few-shot learners. *arXiv preprint arXiv:2005.14165*, 2020. 2
- [5] Rui Chen, Yongwei Chen, Ningxin Jiao, and Kui Jia. Fantasia3d: Disentangling geometry and appearance for high-quality text-to-3d content creation. *arXiv preprint arXiv:2303.13873*, 2023. 3
- [6] Xin Chen, Biao Jiang, Wen Liu, Zilong Huang, Bin Fu, Tao Chen, and Gang Yu. Executing your commands via motion diffusion in latent space. In *Proceedings of the IEEE/CVF Conference on Computer Vision and Pattern Recognition*, pages 18000–18010, 2023. 2, 3
- [7] Zilong Chen, Feng Wang, and Huaping Liu. Text-to-3d using gaussian splatting, 2023. 3
- [8] Seunggeun Chi, Hyung-gun Chi, Hengbo Ma, Nakul Agarwal, Faizan Siddiqui, Karthik Ramani, and Kwonjoon Lee. M2d2m: Multi-motion generation from text with discrete diffusion models. *arXiv preprint arXiv:2407.14502*, 2024. 1, 3
- [9] Rishabh Dabral, Muhammad Hamza Mughal, Vladislav Golyanik, and Christian Theobalt. Mofusion: A framework for denoising-diffusion-based motion synthesis. In *Proceedings of the IEEE/CVF conference on computer vision and pattern recognition*, pages 9760–9770, 2023. 2
- [10] Jacob Devlin. Bert: Pre-training of deep bidirectional transformers for language understanding. *arXiv preprint arXiv:1810.04805*, 2018. 2
- [11] Albert Gu and Tri Dao. Mamba: Linear-time sequence modeling with selective state spaces. *arXiv preprint arXiv:2312.00752*, 2023. 3
- [12] Chuan Guo, Xinxin Zuo, Sen Wang, Shihao Zou, Qingyao Sun, Annan Deng, Minglun Gong, and Li Cheng. Action2motion: Conditioned generation of 3d human motions. In *Proceedings of the 28th ACM International Conference on Multimedia*, pages 2021–2029, 2020. 2, 5
- [13] Chuan Guo, Shihao Zou, Xinxin Zuo, Sen Wang, Wei Ji, Xingyu Li, and Li Cheng. Generating diverse and natural 3d human motions from text. In *Proceedings of the IEEE/CVF Conference on Computer Vision and Pattern Recognition*, pages 5152–5161, 2022. 2, 5, 6, 3
- [14] Chuan Guo, Yuxuan Mu, Muhammad Gohar Javed, Sen Wang, and Li Cheng. Momask: Generative masked modeling of 3d human motions. In *Proceedings of the IEEE/CVF Conference on Computer Vision and Pattern Recognition*, pages 1900–1910, 2024. 2, 3
- [15] Bo Han, Hao Peng, Minjing Dong, Yi Ren, Yixuan Shen, and Chang Xu. Amd: Autoregressive motion diffusion. In *Proceedings of the AAAI Conference on Artificial Intelligence*, pages 2022–2030, 2024. 2, 3
- [16] Amir Hertz, Kfir Aberman, and Daniel Cohen-Or. Delta denoising score. In *Proceedings of the IEEE/CVF International Conference on Computer Vision*, pages 2328–2337, 2023. 3
- [17] Jonathan Ho, Ajay Jain, and Pieter Abbeel. Denoising diffusion probabilistic models. *Advances in neural information processing systems*, 33:6840–6851, 2020. 2
- [18] Daniel Holden, Taku Komura, and Jun Saito. Phase-functioned neural networks for character control. *ACM Transactions on Graphics (TOG)*, 36(4):1–13, 2017. 2
- [19] Yukun Huang, Jianan Wang, Yukai Shi, Xianbiao Qi, Zheng-Jun Zha, and Lei Zhang. Dreamtime: An improved optimization strategy for text-to-3d content creation. *arXiv preprint arXiv:2306.12422*, 2023. 3
- [20] Biao Jiang, Xin Chen, Wen Liu, Jingyi Yu, Gang Yu, and Tao Chen. Motiongpt: Human motion as a foreign language. *Advances in Neural Information Processing Systems*, 36, 2024. 2
- [21] Oren Katzir, Or Patashnik, Daniel Cohen-Or, and Dani Lischinski. Noise-free score distillation. *arXiv preprint arXiv:2310.17590*, 2023. 3
- [22] Bernhard Kerbl, Georgios Kopanas, Thomas Leimkühler, and George Drettakis. 3d gaussian splatting for real-time radiance field rendering. *ACM Transactions on Graphics*, 42(4), 2023. 3
- [23] Taeryung Lee, Gyeongsik Moon, and Kyoung Mu Lee. Multiact: Long-term 3d human motion generation from multiple action labels. In *Proceedings of the AAAI Conference on Artificial Intelligence*, pages 1231–1239, 2023. 1, 2, 3
- [24] Taeryung Lee, Fabien Baradel, Thomas Lucas, Kyoung Mu Lee, and Grégory Rogez. T2lm: Long-term 3d human motion generation from multiple sentences. In *Proceedings of the IEEE/CVF Conference on Computer Vision and Pattern Recognition*, pages 1867–1876, 2024.
- [25] Mengtian Li, Chengshuo Zhai, Shengxiang Yao, Zhifeng Xie, and Keyu Chen Yu-Gang Jiang. Infinite motion: Extended motion generation via long text instructions. *arXiv preprint arXiv:2407.08443*, 2024. 2
- [26] Shuai Li, Sisi Zhuang, Wenfeng Song, Xinyu Zhang, Hejia Chen, and Aimin Hao. Sequential texts driven cohesive motions synthesis with natural transitions. In *Proceedings of the IEEE/CVF International Conference on Computer Vision*, pages 9498–9508, 2023. 2, 3
- [27] Yixun Liang, Xin Yang, Jiantao Lin, Haodong Li, Xiaogang Xu, and Yingcong Chen. Luciddreamer: Towards high-fidelity text-to-3d generation via interval score matching, 2023. 3
- [28] Hung Yu Ling, Fabio Zinno, George Cheng, and Michiel Van De Panne. Character controllers using motion vaes. *ACM Transactions on Graphics (TOG)*, 39(4):40–1, 2020. 2
- [29] Ilya Loshchilov and Frank Hutter. Decoupled weight decay regularization, 2019. 5

- [30] Naureen Mahmood, Nima Ghorbani, Nikolaus F Troje, Gerard Pons-Moll, and Michael J Black. Amass: Archive of motion capture as surface shapes. In *Proceedings of the IEEE/CVF international conference on computer vision*, pages 5442–5451, 2019. 2, 5
- [31] Ben Mildenhall, Pratul P. Srinivasan, Matthew Tancik, Jonathan T. Barron, Ravi Ramamoorthi, and Ren Ng. Nerf: Representing scenes as neural radiance fields for view synthesis, 2020. 3
- [32] Thomas Müller, Alex Evans, Christoph Schied, and Alexander Keller. Instant neural graphics primitives with a multi-resolution hash encoding. *ACM Trans. Graph.*, 41(4):102:1–102:15, 2022. 3
- [33] Alexander Quinn Nichol and Prafulla Dhariwal. Improved denoising diffusion probabilistic models. In *International conference on machine learning*, pages 8162–8171. PMLR, 2021. 2
- [34] Mathis Petrovich, Michael J Black, and Gül Varol. Action-conditioned 3d human motion synthesis with transformer vae. In *Proceedings of the IEEE/CVF International Conference on Computer Vision*, pages 10985–10995, 2021. 5
- [35] Mathis Petrovich, Michael J Black, and Gül Varol. Temos: Generating diverse human motions from textual descriptions. In *European Conference on Computer Vision*, pages 480–497. Springer, 2022. 2
- [36] Matthias Plappert, Christian Mandery, and Tamim Asfour. The kit motion-language dataset. *Big data*, 4(4):236–252, 2016. 2
- [37] Ben Poole, Ajay Jain, Jonathan T Barron, and Ben Mildenhall. Dreamfusion: Text-to-3d using 2d diffusion. *arXiv preprint arXiv:2209.14988*, 2022. 2, 3
- [38] Abhinanda R Punnakkal, Arjun Chandrasekaran, Nikos Athanasiou, Alejandra Quiros-Ramirez, and Michael J Black. Babel: Bodies, action and behavior with english labels. In *Proceedings of the IEEE/CVF Conference on Computer Vision and Pattern Recognition*, pages 722–731, 2021. 2, 5, 6
- [39] Yijun Qian, Jack Urbanek, Alexander G Hauptmann, and Jungdam Won. Breaking the limits of text-conditioned 3d motion synthesis with elaborative descriptions. In *Proceedings of the IEEE/CVF International Conference on Computer Vision*, pages 2306–2316, 2023. 2, 3
- [40] Zhongfei Qing, Zhongang Cai, Zhitao Yang, and Lei Yang. Story-to-motion: Synthesizing infinite and controllable character animation from long text. In *SIGGRAPH Asia 2023 Technical Communications*, pages 1–4. 2023. 3
- [41] Alec Radford, Jong Wook Kim, Chris Hallacy, Aditya Ramesh, Gabriel Goh, Sandhini Agarwal, Girish Sastry, Amanda Askell, Pamela Mishkin, Jack Clark, Gretchen Krueger, and Ilya Sutskever. Learning transferable visual models from natural language supervision, 2021. 2
- [42] Robin Rombach, Andreas Blattmann, Dominik Lorenz, Patrick Esser, and Björn Ommer. High-resolution image synthesis with latent diffusion models. In *Proceedings of the IEEE/CVF conference on computer vision and pattern recognition*, pages 10684–10695, 2022. 3
- [43] Axel Sauer, Dominik Lorenz, Andreas Blattmann, and Robin Rombach. Adversarial diffusion distillation. In *European Conference on Computer Vision*, pages 87–103. Springer, 2025. 3
- [44] Yonatan Shafir, Guy Tevet, Roy Kapon, and Amit H Bermano. Human motion diffusion as a generative prior. *arXiv preprint arXiv:2303.01418*, 2023. 1, 2, 3, 5, 6
- [45] Mingyi Shi, Kfir Aberman, Andreas Aristidou, Taku Komura, Dani Lischinski, Daniel Cohen-Or, and Baoquan Chen. Motionet: 3d human motion reconstruction from monocular video with skeleton consistency. *Acm transactions on graphics (tog)*, 40(1):1–15, 2020. 5
- [46] Jiaming Song, Chenlin Meng, and Stefano Ermon. Denoising diffusion implicit models. *arXiv preprint arXiv:2010.02502*, 2020. 2, 4
- [47] Jiayang Tang, Jiawei Ren, Hang Zhou, Ziwei Liu, and Gang Zeng. Dreamgaussian: Generative gaussian splatting for efficient 3d content creation. *arXiv preprint arXiv:2309.16653*, 2023. 3
- [48] Guy Tevet, Brian Gordon, Amir Hertz, Amit H Bermano, and Daniel Cohen-Or. Motionclip: Exposing human motion generation to clip space. In *European Conference on Computer Vision*, pages 358–374. Springer, 2022. 2
- [49] Guy Tevet, Sigal Raab, Brian Gordon, Yoni Shafir, Daniel Cohen-or, and Amit Haim Bermano. Human motion diffusion model. In *The Eleventh International Conference on Learning Representations*, 2023. 2, 3, 4, 5
- [50] Aaron Van Den Oord, Oriol Vinyals, et al. Neural discrete representation learning. *Advances in neural information processing systems*, 30, 2017. 2
- [51] Haochen Wang, Xiaodan Du, Jiahao Li, Raymond A Yeh, and Greg Shakhnarovich. Score jacobian chaining: Lifting pretrained 2d diffusion models for 3d generation. In *Proceedings of the IEEE/CVF Conference on Computer Vision and Pattern Recognition*, pages 12619–12629, 2023. 3
- [52] Zhengyi Wang, Cheng Lu, Yikai Wang, Fan Bao, Chongxuan Li, Hang Su, and Jun Zhu. Prolificdreamer: High-fidelity and diverse text-to-3d generation with variational score distillation. *Advances in Neural Information Processing Systems*, 36, 2024. 3
- [53] Xiaolin Wei, Peizhao Zhang, and Jinxiang Chai. Accurate real-time full-body motion capture using a single depth camera. *ACM Transactions on Graphics (TOG)*, 31(6):1–12, 2012. 2
- [54] Zhao Yang, Bing Su, and Ji-Rong Wen. Synthesizing long-term human motions with diffusion models via coherent sampling. In *Proceedings of the 31st ACM International Conference on Multimedia*, pages 3954–3964, 2023. 2, 3
- [55] Xin Yu, Yuan-Chen Guo, Yangguang Li, Ding Liang, Song-Hai Zhang, and Xiaojuan Qi. Text-to-3d with classifier score distillation. *arXiv preprint arXiv:2310.19415*, 2023. 3
- [56] Ye Yuan, Jiaming Song, Umar Iqbal, Arash Vahdat, and Jan Kautz. Physdiff: Physics-guided human motion diffusion model. In *Proceedings of the IEEE/CVF international conference on computer vision*, pages 16010–16021, 2023. 2
- [57] Jianrong Zhang, Yangsong Zhang, Xiaodong Cun, Yong Zhang, Hongwei Zhao, Hongtao Lu, Xi Shen, and Ying Shan. Generating human motion from textual descriptions with discrete representations. In *Proceedings of the IEEE/CVF conference on computer vision and pattern recognition*, pages 14730–14740, 2023. 2

- [58] Mingyuan Zhang, Zhongang Cai, Liang Pan, Fangzhou Hong, Xinying Guo, Lei Yang, and Ziwei Liu. Motiandiffuse: Text-driven human motion generation with diffusion model. *arXiv preprint arXiv:2208.15001*, 2022. 3
- [59] Mingyuan Zhang, Xinying Guo, Liang Pan, Zhongang Cai, Fangzhou Hong, Huirong Li, Lei Yang, and Ziwei Liu. Remodiffuse: Retrieval-augmented motion diffusion model. In *Proceedings of the IEEE/CVF International Conference on Computer Vision*, pages 364–373, 2023. 2
- [60] Mingyuan Zhang, Huirong Li, Zhongang Cai, Jiawei Ren, Lei Yang, and Ziwei Liu. Finemogen: Fine-grained spatio-temporal motion generation and editing. *Advances in Neural Information Processing Systems*, 36:13981–13992, 2023. 2
- [61] Qinsheng Zhang, Jiaming Song, Xun Huang, Yongxin Chen, and Ming-Yu Liu. Diffcollage: Parallel generation of large content with diffusion models. In *2023 IEEE/CVF Conference on Computer Vision and Pattern Recognition (CVPR)*, pages 10188–10198. IEEE, 2023. 2, 6
- [62] Yan Zhang, Michael J Black, and Siyu Tang. Perpetual motion: Generating unbounded human motion. *arXiv preprint arXiv:2007.13886*, 2020. 1, 3
- [63] Zeyu Zhang, Akide Liu, Qi Chen, Feng Chen, Ian Reid, Richard Hartley, Bohan Zhuang, and Hao Tang. Infinimotion: Mamba boosts memory in transformer for arbitrary long motion generation. *arXiv preprint arXiv:2407.10061*, 2024.
- [64] Zeyu Zhang, Akide Liu, Ian Reid, Richard Hartley, Bohan Zhuang, and Hao Tang. Motion mamba: Efficient and long sequence motion generation with hierarchical and bidirectional selective ssm. *arXiv preprint arXiv:2403.07487*, 2024. 3
- [65] Chongyang Zhong, Lei Hu, Zihao Zhang, and Shihong Xia. Attt2m: Text-driven human motion generation with multi-perspective attention mechanism. In *Proceedings of the IEEE/CVF International Conference on Computer Vision*, pages 509–519, 2023. 2
- [66] Joseph Zhu and Peiye Zhuang. Hifa: High-fidelity text-to-3d with advanced diffusion guidance. *arXiv preprint arXiv:2305.18766*, 2023. 3
- [67] Lianghan Zhu, Yanqi Bao, Jing Huo, Jing Wu, Yu-Kun Lai, Wenbin Li, and Yang Gao. Zero-shot video editing through adaptive sliding score distillation. *arXiv preprint arXiv:2406.04888*, 2024. 3

A. Theoretical Analysis: Segment Score Distillation and Global Consistency

We provide a theoretical analysis to demonstrate that if the Segment Score Distillation loss $\mathcal{L}_{align} = \mathbb{E}_{t,\epsilon} [w(t) \|\hat{x}_0^i - x_0^i\|_2^2]$ converges, the resulting long motion sequence M is guaranteed to be globally coherent and smooth.

A.1. Problem Setup

Let $M = \{m_1, t_1, m_2, t_2, \dots, m_N\}$ denote a long motion sequence M , where m_i represents the motion segment corresponding to the i -th text prompt, and t_i represents the transition segment between m_i and m_{i+1} . The initial sequence M is constructed by concatenating motion segments $\{m_i\}$ with randomly initialized transition $\{t_i\}$. Our goal is to iteratively optimize M so that:

- (i) Each motion segment m_i and transition t_i conforms to a learned motion prior $p(x)$, ensuring realism.
- (ii) M achieves global coherence and smoothness.

To optimize M , we introduce Segment Score Distillation (SSD), which operates as follows:

- (i) Using a sliding window, we sample overlapping short sequences $\{x_0^i\}_{i=1}^K$ from M , where each $x_0^i = M[i : i + L]$ spans motion segments (m_i, m_{i+1} and transitions (t_i).
- (ii) Add noise to each sampled sequence to obtain $x_t^i \sim q(x_t^i | x_0^i)$.
- (iii) Denoise x_t^i using the Motion Diffusion Model ϕ to predict \hat{x}_0^i , and compute the alignment loss:

$$\mathcal{L}_{align} = \mathbf{E}_{t,\epsilon} [w(t) \|\hat{x}_0^i - x_0^i\|_2^2], \quad (8)$$

- (iv) The loss \mathcal{L}_{align} is back-propagated to optimize M , ensuring that both m_i and t_i align with $p(x)$

A.2. Theoretical Analysis

We now prove that minimizing \mathcal{L}_{align} ensures global coherence and smoothness in M .

A.2.1. Local Consistency Through Loss Convergence

The Motion Diffusion Model ϕ is trained to model the conditional distribution of motion x_0^i at time step t :

$$\hat{x}_0^i = \phi(x_t^i, t), \quad x_t^i \sim q(x_t^i | x_0^i), \quad (9)$$

where $q(x_t^i | x_0^i)$ represents the forward diffusion process.

When $\mathcal{L}_{align} \rightarrow 0$, the predicted \hat{x}_0^i aligns with the x_0^i for all sampled segments. This implies:

- (i) Each segment x_0^i conforms to the motion prior $p(x)$, which encodes realistic and smooth dynamics.
- (ii) The transitions within x_0^i are temporally consistent.

A.2.2. Global Coherence via Overlapping Optimization

The sliding window mechanism ensures that adjacent sampled sequences overlap. Let:

$$x_0^i = M[i : i + L], \quad x_0^{i+1} = M[i + \delta : i + L + \delta], \quad (10)$$

where L is the segment length, and δ is the overlap step size. The overlapping region $O^i = x_0^i \cap x_0^{i+1}$ satisfies:

$$\hat{x}_0^i[O^i] \rightarrow x_0^i[O^i], \quad \hat{x}_0^{i+1}[O^i] \rightarrow x_0^{i+1}[O^i], \quad (11)$$

by transitivity:

$$\|\hat{x}_0^i[O^i] - \hat{x}_0^{i+1}[O^i]\|_2^2 \rightarrow 0, \quad (12)$$

as $\mathcal{L}_{align} \rightarrow 0$. By enforcing consistency within overlapping regions, the optimization propagates coherence across the entire sequence M .

A.2.3. Smoothness Guarantee

Smoothness in M is ensured through two mechanisms:

(1) **Local Smoothness:** The loss \mathcal{L}_{align} minimizes the discrepancy between \hat{x}_0^i and x_0^i , ensuring smooth dynamics within each short segment.

(2) **Global Smoothness:** Overlapping regions O^i propagate smoothness across segment boundaries.

By the end of optimization, all segments and transitions are aligned with $p(x)$, resulting in a globally smooth sequence M .

B. Further implementation details

To facilitate better reproducibility of our work, we provide additional details about our implementation in this section. For HumanML3D, we set the fps as 20, and encode timesteps as a sinusoidal positional encoding. We utilize a dense layer to encode poses of 263D into a sequence of 512D vectors. For BABEL, we set fps as 30. We encode poses of 135D into a sequence of 512D vectors. In the first stage, we utilize guidance scale 2.5 to generate each single motion segments, and in the process of Segment Score Distillation, we utilize 7.5 to optimize the entire motion sequence. We set the weighting function $w(t)$ as $1 - \alpha(t)$ for all experiments.

C. More experimental results

In this section, we present more experimental results to validate the effectiveness of our framework.

C.1. More quantitative results

We also compare our framework with the latest work, FlowMDM [3], which introduces Blended Positional Encodings, a technique that combines absolute and relative positional encodings in the denoising process. We follow the evaluation protocol of FlowMDM [3]. However, we only use FlowMDM [3] to generate individual motion segments,

	Motion				Transition			
	R-prec \uparrow	FID \downarrow	Div \rightarrow	MM-Dist \downarrow	FID \downarrow	Div \rightarrow	PJ \rightarrow	AUJ \downarrow
Ground Truth	0.796 \pm 0.004	0.00 \pm 0.00	9.34 \pm 0.08	2.97 \pm 0.01	0.00 \pm 0.00	9.54 \pm 0.15	0.02 \pm 0.00	0.00 \pm 0.00
DoubleTake*	0.643 $^{\pm 0.005}$	0.80 $^{\pm 0.02}$	9.20 $^{\pm 0.11}$	3.92 $^{\pm 0.01}$	1.71 $^{\pm 0.05}$	8.82 $^{\pm 0.13}$	0.52 $^{\pm 0.01}$	2.10 $^{\pm 0.03}$
DoubleTake	0.628 $^{\pm 0.005}$	1.25 $^{\pm 0.04}$	9.09 $^{\pm 0.12}$	4.01 $^{\pm 0.01}$	4.19 $^{\pm 0.09}$	8.45 $^{\pm 0.09}$	0.48 $^{\pm 0.00}$	1.83 $^{\pm 0.02}$
MultiDiffusion	0.629 $^{\pm 0.002}$	1.19 $^{\pm 0.03}$	9.38 $^{\pm 0.08}$	4.02 $^{\pm 0.01}$	4.31 $^{\pm 0.06}$	8.37 $^{\pm 0.10}$	<u>0.17</u> $^{\pm 0.00}$	<u>1.06</u> $^{\pm 0.01}$
DiffCollage	0.615 $^{\pm 0.005}$	1.56 $^{\pm 0.04}$	8.79 $^{\pm 0.08}$	4.13 $^{\pm 0.02}$	4.59 $^{\pm 0.10}$	8.22 $^{\pm 0.11}$	0.26 $^{\pm 0.00}$	2.85 $^{\pm 0.09}$
FlowMDM	0.685 $^{\pm 0.004}$	0.29 $^{\pm 0.01}$	9.58 $^{\pm 0.12}$	3.61 $^{\pm 0.01}$	1.38 $^{\pm 0.05}$	<u>8.79</u> $^{\pm 0.09}$	0.06 $^{\pm 0.00}$	0.51 $^{\pm 0.01}$
InfiniDreamer (ours)	<u>0.674</u> $^{\pm 0.004}$	<u>0.68</u> $^{\pm 0.02}$	<u>9.27</u> $^{\pm 0.11}$	<u>3.78</u> $^{\pm 0.01}$	<u>1.64</u> $^{\pm 0.05}$	8.77 $^{\pm 0.11}$	0.31 $^{\pm 0.00}$	1.49 $^{\pm 0.01}$

Table 4. Comparison of InfiniDreamer with the state of the art in HumanML3D. Symbols \uparrow , \downarrow , and \rightarrow mean that higher, lower, or closer to the ground truth (GT) value are better, respectively. We run each evaluation 10 times to obtain the final results. We use **Bold** to indicate the best result, and use underline to indicate the second-best result.

	Motion				Transition			
	R-prec \uparrow	FID \downarrow	Div \rightarrow	MM-Dist \downarrow	FID \downarrow	Div \rightarrow	PJ \rightarrow	AUJ \downarrow
Ground Truth	0.715 $^{\pm 0.003}$	0.00 $^{\pm 0.00}$	8.42 $^{\pm 0.15}$	3.36 $^{\pm 0.00}$	0.00 $^{\pm 0.00}$	6.20 $^{\pm 0.06}$	0.02 $^{\pm 0.00}$	0.00 $^{\pm 0.00}$
TEACH_B	0.703 $^{\pm 0.002}$	1.71 $^{\pm 0.03}$	8.18 $^{\pm 0.14}$	3.43 $^{\pm 0.01}$	3.01 $^{\pm 0.04}$	6.23 $^{\pm 0.05}$	1.09 $^{\pm 0.00}$	2.35 $^{\pm 0.01}$
TEACH	0.655 $^{\pm 0.002}$	1.82 $^{\pm 0.02}$	7.96 $^{\pm 0.11}$	3.72 $^{\pm 0.01}$	3.27 $^{\pm 0.04}$	6.14 $^{\pm 0.06}$	<u>0.07</u> $^{\pm 0.00}$	<u>0.44</u> $^{\pm 0.00}$
DoubleTake*	0.596 $^{\pm 0.005}$	3.16 $^{\pm 0.06}$	7.53 $^{\pm 0.11}$	4.17 $^{\pm 0.02}$	3.33 $^{\pm 0.06}$	<u>6.16</u> $^{\pm 0.05}$	0.28 $^{\pm 0.00}$	1.04 $^{\pm 0.01}$
DoubleTake	0.668 $^{\pm 0.005}$	<u>1.33</u> $^{\pm 0.04}$	7.98 $^{\pm 0.12}$	3.67 $^{\pm 0.03}$	3.15 $^{\pm 0.05}$	6.14 $^{\pm 0.07}$	0.17 $^{\pm 0.00}$	0.64 $^{\pm 0.01}$
MultiDiffusion	<u>0.702</u> $^{\pm 0.005}$	1.74 $^{\pm 0.04}$	8.37 $^{\pm 0.13}$	3.43 $^{\pm 0.02}$	6.56 $^{\pm 0.12}$	5.72 $^{\pm 0.07}$	0.18 $^{\pm 0.00}$	0.68 $^{\pm 0.00}$
DiffCollage	0.671 $^{\pm 0.003}$	1.45 $^{\pm 0.05}$	7.93 $^{\pm 0.09}$	3.71 $^{\pm 0.01}$	4.36 $^{\pm 0.09}$	6.09 $^{\pm 0.08}$	0.19 $^{\pm 0.00}$	0.84 $^{\pm 0.01}$
FlowMDM	<u>0.702</u> $^{\pm 0.004}$	0.99 $^{\pm 0.04}$	<u>8.36</u> $^{\pm 0.13}$	3.45 $^{\pm 0.02}$	2.61 $^{\pm 0.06}$	6.47 $^{\pm 0.05}$	0.06 $^{\pm 0.00}$	0.13 $^{\pm 0.00}$
InfiniDreamer (ours)	0.667 $^{\pm 0.005}$	1.49 $^{\pm 0.03}$	7.94 $^{\pm 0.14}$	3.53 $^{\pm 0.01}$	<u>2.97</u> $^{\pm 0.08}$	6.31 $^{\pm 0.07}$	0.19 $^{\pm 0.00}$	0.64 $^{\pm 0.01}$

Table 5. Comparison of InfiniDreamer with the state of the art in BABEL. Symbols \uparrow , \downarrow , and \rightarrow mean that higher, lower, or closer to the ground truth (GT) value are better, respectively. We run each evaluation 10 times to obtain the final results. We use **Bold** to indicate the best result, and use underline to indicate the second-best result.

and then use our method to generate the entire long motion sequence. As shown in Tab. 4 and Tab. 5, we find that InfiniDreamer performs slightly worse than FlowMDM [3] but outperforms previous training-free methods. We speculate that this is because FlowMDM [3] is fine-tuned on long human motion sequences using both absolute and relative positional encodings, which introduces some interference in individual short motion segments. Our method, which adds further interference, therefore achieves slightly lower performance compared to FlowMDM [3]. Nonetheless, the experimental results demonstrate the advantages of our approach over DoubleTake [44].

C.2. More qualitative results

We also conducted qualitative experiments to compare the results of our framework with those of FlowMDM [3]. In this section, we use the open-source model of FlowMDM [3] to generate its results, while for our method, we use MDM [49] as our motion prior. As shown in Fig. 5,

we present two examples of long motion sequence generation. The first example, at the top of the figure, is generated using the text prompts ‘jogging forward slowly’ + ‘a person is walking down the stairs’ + ‘jogging forward slowly’. The results show that both FlowMDM and our method can infer the transitional ‘walking up the stairs’ segment before descending. However, FlowMDM exhibits slight motion drift during this segment. In the second example, with the text prompts ‘a person is walking straight’ + ‘side steps’ + ‘he is walking backward’, we observe that FlowMDM generates the ‘side steps’ motion incorrectly and also shows motion drift at the end. In contrast, our method avoids these issues, producing more accurate and coherent results. Additionally, we observe that the motions generated by FlowMDM exhibit a larger displacement range, while our method produces smoother and more controlled movements.

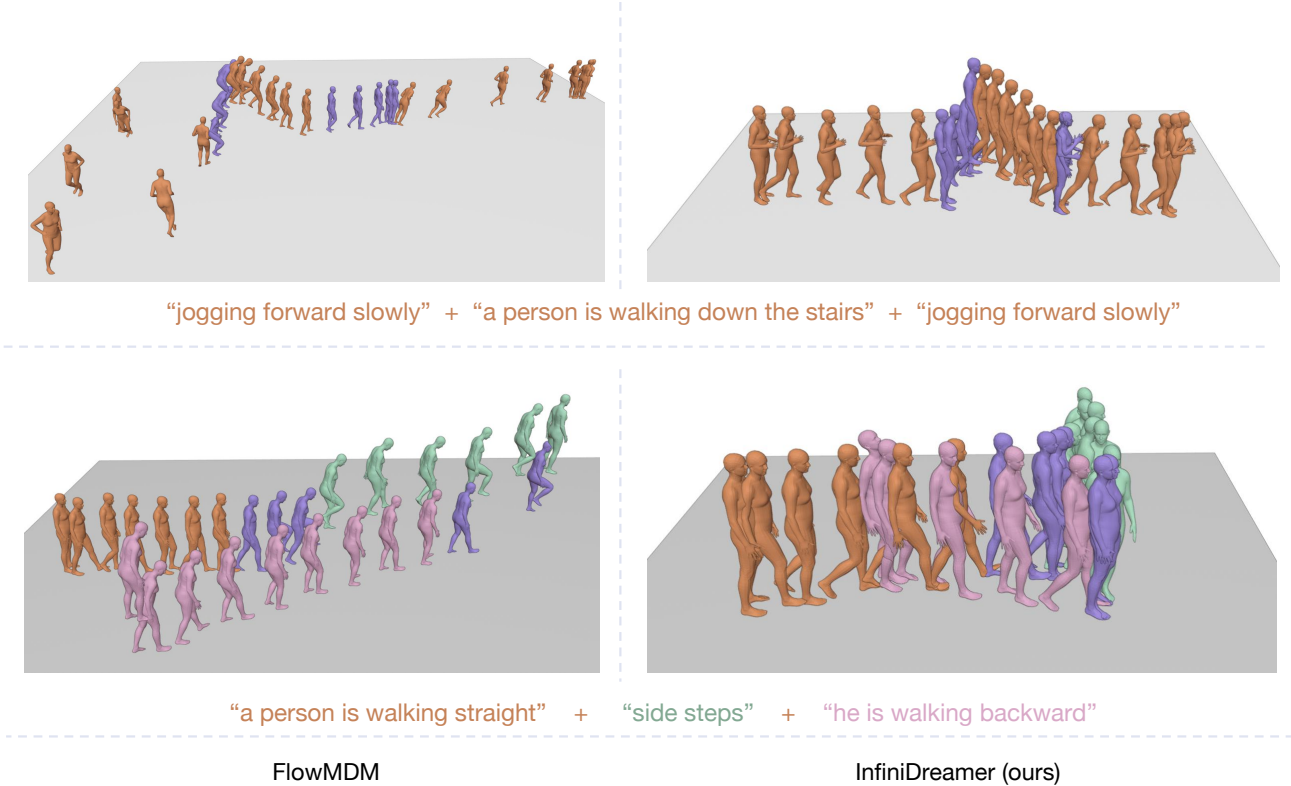


Figure 5. Qualitative Comparisons to FlowMDM for Long Motion Generation. We present two examples: in the top row, our framework demonstrates strong contextual understanding, guiding the transition segment to “go upstairs” in response to the following “downstairs” prompt. In contrast, FlowMDM shows slightly motion drift in this segment. In the bottom row, we use a more fine-grained textual prompt, where the FlowMDM exhibits issues with motion drift and semantic errors, failing to generate the “side steps” segment. Our framework, however, produces a higher-quality sequence with enhanced fine-grained comprehension of the text.

	Motion				Transition (30 frames)	
	R-precision \uparrow	FID \downarrow	Diversity \rightarrow	MultiModal-Dist \downarrow	FID \downarrow	Diversity \rightarrow
Ground Truth	0.797 ± 0.003	$1.6 \cdot 10^{-3} \pm 0.00$	9.59 ± 0.13	2.98 ± 0.01	$1.8 \cdot 10^{-3} \pm 0.00$	9.55 ± 0.09
InfiniDreamer	0.627 ± 0.009	0.62 ± 0.07	<u>9.60 ± 0.15</u>	3.37 ± 0.01	2.43 ± 0.30	8.44 ± 0.09
+‘transition’	<u>0.624 ± 0.010</u>	<u>0.65 ± 0.06</u>	9.59 ± 0.11	<u>3.38 ± 0.01</u>	<u>2.45 ± 0.28</u>	<u>8.45 ± 0.09</u>
+‘motion’	0.615 ± 0.012	0.71 ± 0.09	9.63 ± 0.13	3.42 ± 0.01	2.52 ± 0.33	8.53 ± 0.11

Table 6. Ablation Study on textual prompt. We use different textual prompt as our text condition. We find that text prompts has a negative impact on InfiniDreamer. When using ‘transition’ as the text prompt, the model performance slightly decreases, and when using ‘motion’ as the text prompt, the performance drops significantly. We believe this is because the text prompts used are not well-suited to capture the semantics of diverse transition segments. Therefore, in our baseline, we adopt the unconditional mode for optimization.

C.3. More ablation study on prompts

In this section, we present additional ablation studies. We explore the use of different text conditions to guide the optimization of Segment Score Distillation (SSD). In the original experiments, we optimized in an unconditional manner. Here, we use text prompts such as “transition” and “motion” as conditions, with a guidance scale of 7.5 applied during optimization. We conduct our ablation studies on the Hu-

manML3D [13] dataset. As shown in Tab. 6, we observe that incorporating text prompts negatively affects the performance of InfiniDreamer. Using ‘transition’ as a prompt leads to a slight performance decline, while ‘motion’ causes a more significant drop. We believe this is because the chosen text prompts are struggle to capture the semantic diversity of various transition segments. Therefore, we opted for an unconditional model in our baseline.

mance by advancing the capabilities of the short-sequence generation model.

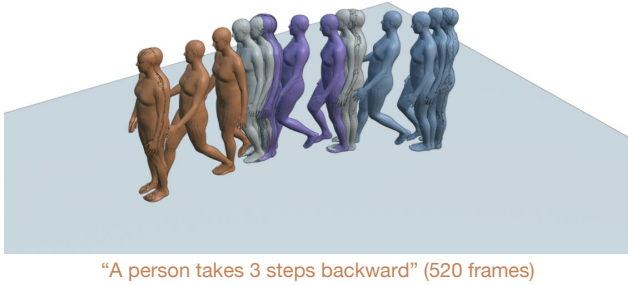


Figure 6. We demonstrate InfiniDreamer’s capability to generate long motion sequence from a single text prompt. Starting with a base model designed to generate short sequences (approximately 70 to 200 frames), our framework extends its generation range to 520 frames while ensuring that the generated motions remain semantically consistent with the input text.

C.4. Long motion generation with Single Prompt

Our framework has an additional capability: it can generate long motion sequences from a single text prompt. It is a feature that currently beyond the reach of other models. Specifically, given a short-sequence generation model, Motion Diffusion Model (MDM) [49], we set the total frame count of the long sequence to 520 frames and the frame count of each short sequence to 120 frames. We employ conditional Segment Score Distillation (SSD), using the text prompt as the conditioning input. At the beginning, we randomly initialize a long motion sequence. In this experiment, we omit the first stage of InfiniDreamer, meaning that we do not use MDM to generate the initial short motion sequence. In the subsequent stages, we set the guidance scale to 10.0 and the learning rate to 0.005. As shown in Fig. 6, we use “a person takes 3 steps backward” as our textual prompt. InfiniDreamer, through conditional optimization, extends the generation capability of the original Motion Diffusion Model (MDM) from 70-200 frames to 520 frames, while maintaining alignment between the generated motions and the input text.

D. Limitation

InfiniDreamer is capable of generating arbitrarily long motion sequences based on text prompts, even in single-text scenarios. However, our framework still has some limitations. For example, the generation of sub-motions is constrained by the performance of the short-sequence generation model. Additionally, our method is slower compared to other sampling approaches, taking approximately 4 minutes to generate a 520-frame sequence. In the future, we plan to improve its efficiency and enhance InfiniDreamer’s perfor-